IEEE Access
Multidisciplinary | Rapid Review | Open Access Journal

Received December 10, 2017, accepted January 23, 2018, date of publication February 5, 2018, date of current version March 19, 2018.

Digital Object Identifier 10.1109/ACCESS.2018.2802379

Focusing Microwaves in the Fresnel Zone With a Cavity-Backed Holographic Metasurface

VINAY R. GOWDA, MOHAMMADREZA F. IMANI, (Member, IEEE), TIMOTHY SLEASMAN, (Student Member, IEEE), OKAN YURDUSEVEN, (Senior Member, IEEE), AND DAVID R. SMITH, (Member, IEEE)

Center for Metamaterials and Integrated Plasmonics, Department of Electrical and Computer Engineering, Duke University, Durham, NC 27708, USA.

Corresponding author: Vinay R. Gowda (vinay.ramachandra.gowda@duke.edu)

This work was supported by the Air Force Office of Scientific Research under Grant FA9550-12-1-0491.

ABSTRACT We present the design and experimental demonstration of a cavity-backed, holographic metasurface capable of focusing microwaves in the Fresnel zone. The circular cavity consists of two stacked plates: microwaves are injected into the bottom plate via a coaxial connector, which forms the feed layer, and are coupled to the top holographic metasurface layer via an annular ring on the periphery of the cavity. This coupling results in an inward traveling cylindrical wave in the top layer, which serves as the reference wave for the hologram. A sparse array of slots, patterned into the upper plate, constitutes the hologram that produces the focal spot. To mitigate high sidelobe levels and improve performance, a tapered design, facilitated by varying the slot size, is also introduced. The proposed designs—which have a 10-cm diameter, operate at 20 GHz, and form a focal spot at a distance of 10 cm—are validated using full-wave simulations as well as measurements of fabricated samples. The proposed focusing metasurface may find application as a compact source for Fresnel zone wireless power transfer and remote sensing schemes.

INDEX TERMS Focusing, Fresnel zone, cavity-backed, holography, metasurfaces, microwaves.

I. INTRODUCTION

Apertures that focus microwave energy in the Fresnel zone (sometimes referred to as the radiative near-field, where $d < 2D^2/\lambda_0$, D is the aperture dimension, λ_0 is the free space operating wavelength, and d is the distance from the antenna) are of interest for a variety of applications such as medical imaging and therapy [1], remote sensing [2], [3] and wireless power transfer [4], [5]. For example, Fresnel zone focusing is vital to achieving microwave-induced hyperthermia [6], where electromagnetic fields are confined to cancerous regions without harming nearby tissue. Focusing antennas have also gained traction for wireless charging of biomedical implants [4], [5]. In remote sensing [2], [3] focusing apertures are essential to provide precise sensing information (for example, the temperature of food products in a production facility) without direct contact.

Among the many applications of focusing electromagnetic waves, wireless power transfer—a century-old concept pioneered by Tesla [7]—has been of considerable interest recently. Modern approaches have largely been dominated by schemes involving inductive coupling between resonators [8], [9], which severely restricts power transfer to short (near contact) operating distances. Interest in wireless power transfer was revived about a decade ago by the work of Kurs *et al.* [8] where the authors showed that the operating distance can be increased by employing coupled resonators [9], [10]. More recently, it was shown that opportunity exists for wireless power transfer at even larger operating distances by employing Fresnel zone focusing [11]–[14], which is particularly necessary in applications where the required separation between the source and receiver precludes inductive, near-field approaches. Structures like patch antenna arrays, retro-directive arrays, and corrugated waveguides have been pursued as a means for focusing electromagnetic fields in the Fresnel zone for power transfer applications [15]–[19]. However, such structures usually result in complicated feed networks, in the case of patch arrays, and unfavorable configurations for realizing dynamic beamforming, in the case of corrugated structures. Forming a local hotspot by shaping the waveforms in a large cavity [20], [21] and using a MIMO configuration [22] have also been proposed.

A systematic approach to the design of a Fresnel zone wireless power transfer aperture follows naturally from the basic

principles of holography [13]. In this framework, a hologram is designed to form a focal spot at a desired location under the excitation of a reference wave. The hologram is formed by implementing a phase distribution that results from the interference of the back propagated focusing field and the field of the reference wave over a planar surface. From the perspective of antenna engineering, such a Fresnel zone focusing aperture supports a field (or current) distribution that constructively interferes at a spot within the Fresnel zone. Over the years, various approaches have been proposed to realize such focusing apertures that can be dynamically reconfigured. One approach is that of phased arrays or electronically scanned antennas (ESAs), which consist of arrays of independently tunable antenna elements. The amplitude and phase of each element can be varied to produce virtually arbitrary aperture field distributions, including those required for Fresnel focusing. Passive phased arrays make use of a single microwave source that is subdivided via a feed network to the radiating elements, each of which has a phase shifter [23], [24]. This sets the phase of each radiating site, much like in the case of a phase hologram. ESAs consist of arrays of transmit modules, each containing a phase shifter as well as one or more amplifiers, which enable arbitrary waveforms to be synthesized [25]. Use of such structures provides enough degrees of freedom to generate any desired aperture distribution; however, this comprehensive control comes at the cost of hardware complexity. In the passive case, the feed network can become complicated as the aperture size grows. In either the passive or active case the cost, high power consumption of phase shifters and amplifiers, and other complications associated with arrays of active components can be barriers for many potential applications [23], [24].

Particularly for narrowband applications, an alternative to phased arrays and ESAs are quasi-optical lenses such as Fresnel zone plates [26], [27]. These plates are illuminated by a source in the near field of the aperture and are patterned to form a focal spot on the opposite side of the plate (in transmission mode). While the focal spots produced by this approach are promising, the device has a large form factor—due to the use of free space propagation—that may not be suitable in many scenarios. The architecture proposed in [27] also relied on mechanical motion to provide beam steering. More recently, near-field focusing plates and leaky-wave antennas have been proposed and have experimentally demonstrated the ability to generate focal spots [28]–[36]. However, the operating distance of near-field focusing plates is usually limited due to the confined nature of the reactive near field. Most leaky-wave antenna designs generate a focal pattern consisting of a longitudinal electric field, which significantly complicates receiver design and does not have a favorable form factor [36]. In [28], a leaky-wave antenna was designed to generate a circularly polarized focal spot, but its ability to shift the focal point along the range direction was reliant on changing the driving frequency. Dependence on frequency to produce distinct radiation patterns severely complicates the source and detector circuitry. In a similar manner, the authors' in [34] present a holographic, radially-polarized, annular leaky wave antenna for Fresnel zone focusing; however, the annular slots used in [34] do not offer an easy path to a reconfigurable aperture. Furthermore, similar to the device presented in [28], the generated focal spot consists of a longitudinal electric field, which complicates receiver design.

Metasurface design concepts provide a simple and efficient avenue for realizing the desired hologram for focusing applications. One particularly attractive version of a metasurface antenna consists of an array of metamaterial resonators excited by a guided mode. Each metamaterial element leaks a portion of the guided wave into free space [37]. The overall radiation pattern is thus the superposition of the contributions from each element. By properly designing the electromagnetic response of each metamaterial element (for example by altering their geometrical properties), waveforms with desired characteristics can be sculpted. Metasurface antennas [38]–[40] have low manufacturing costs and planar form-factors, making them suitable candidates for applications related to beamforming and wavefront shaping. While arbitrary control over the phase and amplitude of each radiating element is not easily obtained in this metasurface architecture, sufficient control can be achieved to enable focusing using a variety of phase and/or amplitude holographic design approaches [41]–[43].

In [13], the general concept of using metasurface holograms for focusing electromagnetic waves and wireless power transfer was investigated in detail. Here, we design and implement a holographic metasurface aperture that can generate focal spots at prescribed locations in the Fresnel zone. The proposed design is a dual-layer cavity which consists of a holographic metasurface layer and a feed layer, as depicted in Fig. 1. The reference wave of the hologram is the guided mode of the planar waveguide structure rather than a plane wave excitation (as in [43]), making the entire structure highly compact. A pattern of slots on the metasurface layer of the structure serves as the hologram, allowing microwaves to radiate out of the cavity and form a focus at desired locations. The holographic pattern is formed from the interference of the field from a hypothetical point source (located at the desired focal spot) backpropagated to the aperture plane, with the reference mode of the cavity. The hologram is realized by carefully positioning slots, placed in such a manner that the hologram field distribution is well approximated. When the slots are excited by the guided mode of the cavity, a diffraction-limited focus is produced at the position of the hypothetical point source.

The dual-layer structure depicted in Fig. 1 is a well-known structure in antenna engineering. It is usually referred to as a radial line slot array (RLSA) and its characteristics and design process are well established in the literature [44]–[46]. Single and dual layer designs have been presented, both of which have mainly been used to generate a directive far field beam at desired directions. These designs were initially proposed for satellite communication. We utilize the

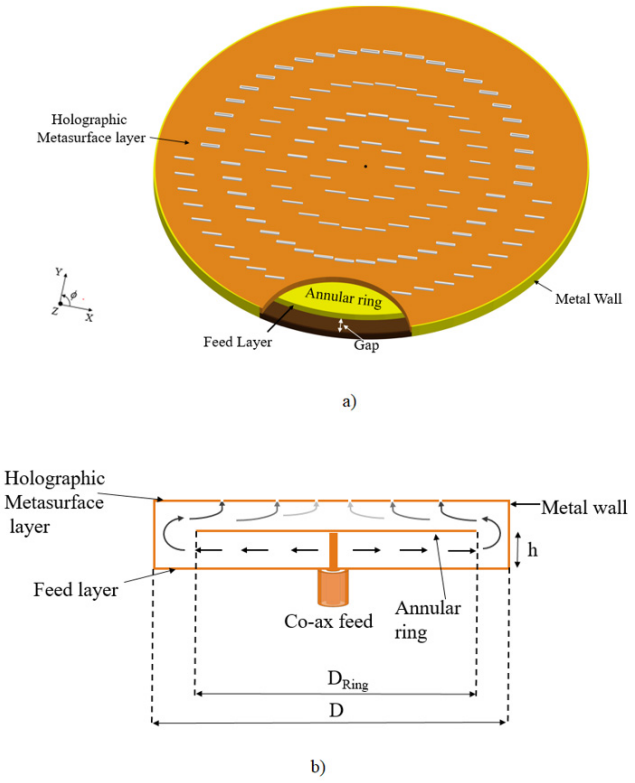

FIGURE 1. **An Illustration of the focused metasurface aperture (a) cross-sectional view (b) side view.**

RLSA configuration here because it ensures high aperture efficiency; the RLSA has a converging wave pattern which balances the substrate/radiation losses to create a more uniform aperture distribution [44], [45]. The high efficiency of the RLSA can be contrasted with that of a single parallel plate waveguide, in which the outward-traveling cylindrical wave rapidly decays as a function of radius and excites only a small portion of the aperture. The dual layer structure used here effectively provides a circumferentially uniform feed, creating an incoming cylindrical wave. Furthermore, the rate of leakage, or *coupling strength*, of each element can be varied as a function of radius to harness further control over the energy radiated by the device [47]–[50]. Such a tapering of the aperture's radiating sources can be used to reduce sidelobe levels.

In this paper, we describe the operation of the proposed dual-layer holographic metasurface and outline its design procedure. Full-wave simulations and experimental results confirming the proposed design's operation are presented. Samples with and without tapered coupling strengths are demonstrated and a reduction in sidelobe level is observed as a result of the tapering. We also discuss the tradeoffs governing the size of the aperture and their impacts on the focal spot characteristics. The proposed design creates a focus with a linear polarization, but a focus in both polarizations could be achieved by patterning the hologram with different element orientations—a prospect which is beyond the scope of this paper and will be examined in future works. While we present only passive designs here, we note that the proposed architecture is compact, planar, and can be made reconfigurable by introducing independently-addressable switchable components, such as diodes, into each radiator [51], [52]. The passive holographic aperture, nevertheless, represents a step in the direction of creating a compact source aperture that can produce focused fields in the Fresnel zone—one of the key components of the ultimate wireless power system envisioned in [13].

II. DUAL-LAYER METASURFACE HOLOGRAM DESIGN

Figure 1 shows the cross-sectional and side view of the proposed cavity-backed metasurface aperture. The dual layer cavity design consists of a feed layer and a holographic metasurface layer. Microwaves are injected into the bottom plate through a coaxial adaptor and are coupled into the above metasurface layer—patterned with carefully arranged radiating slots—via an annular ring on the periphery of the cavity. The diameter of the entire structure is D. The annular ring connecting the two layers, as shown in Fig. 1 (a), has an inner diameter of D_{Ring} and the outer diameter is the edge of the cavity. This leaves a gap of (D - D_{Ring})/2 from the metal wall, allowing the microwaves to be coupled from the feed layer to the holographic metasurface layer. The appropriate size for the annular ring was selected by running a parametric sweep in a full-wave solver to minimize reflection at the desired frequency of 20 GHz ($|S_{11}| < -10$ dB). The thickness of the waveguide is selected to be less than $h < \lambda_g/2$ so that only a single mode is supported in the cavity-backed structure.

To design the focusing metasurface hologram, the first step is to select our desired focal spot $F(x_0, y_0, z_0)$ located in the Fresnel region. To further simplify the problem, we want the fields at the focus to form a linearly polarized electric field along the y-direction. In the next step, we backpropagate the fields from a hypothetical point source at the focal spot to the aperture to determine the fields on the hologram plane. The reference wave within the waveguide is multiplied by the complex conjugate of the desired field distribution on the aperture to obtain a hologram, which ideally creates the radiating sources with the correct phase and magnitude to form the desired spot. Since the metasurface architecture we employ (a distribution of simple slots) does not allow for independent control over phase and amplitude at each point in the aperture, we focus on reproducing the phase the hologram, which predominantly governs the performance of the hologram. The result of multiplying the point source fields with the reference wave (the inward-traveling cylindrical wave) is thus a distribution of phase values that range between 0 and 2π. Our available phase values to realize this phase hologram are due to two factors: the guided mode and the response of each of the elements. Because the phase introduced by the slots is generally constrained to a narrow set of values, we only make use of the phase associated with the propagation of the guided mode. At locations where the

phase difference between the desired focusing hologram and the guided mode is less than a threshold value a radiating slot is placed. Although the phase is utilized to form the hologram, we will later implement a taper on the aperture to create an amplitude window which mitigates large sidelobe levels. In future works, the use of subwavelength metamaterial elements with dynamically tunable properties [51], [52] can enable further control over the phase and magnitude distribution on the aperture.

Elongated slots are used as radiating elements in the metasurface aperture in this paper. Such elements guarantee that the radiated fields exhibit the desired linear polarization. Given the subwavelength width of the slots, they can be modeled as magnetic dipoles polarized along their lengthwise axis [53], [54]. As a result, only magnetic fields parallel to the length dimension can excite the slots. Given our goal to form focal spots with a y-polarized field, we only use the x component of the magnetic field of the reference wave (inward-traveling cylindrical wave) in our calculations of the hologram. The x component of this field is given by the Hankel function of the first kind [55] (assuming $e^{-i\omega t}$ convention):

$$H_x = H_1^{(1)}(k\rho)\cos(\phi) \tag{1}$$

where $\rho = \sqrt{x^2 + y^2}$, k is the wavenumber within the waveguide, and ϕ is the azimuth angle in the aperture plane (x-y) measured from the x-axis (see Fig. 1). Considering the center of the aperture as the origin of the coordinate system, a point source located at $F(x_0, y_0, z_0)$ will generate fields on the aperture, which are given by:

$$E\,(x, y, 0) \propto \frac{e^{ik\sqrt{(x-x_0)^2+(y-y_0)^2+z_0^2}}}{\sqrt{(x-x_0)^2 + (y-y_0)^2 + z_0^2}} \tag{2}$$

The reference wave is divided by the fields from the point source on the aperture plane, E, to produce a hologram which, when stimulated by the inward traveling cylindrical wave, will result in a diffraction-limited focused spot at the location $F(x_0, y_0, z_0)$. Since our goal is to generate a phase hologram, we only insert slots in the hologram at locations where the phase difference is below a tolerance, as found from

$$U = \angle H_x - \angle E(x, y, 0). \tag{3}$$

In the calculation of the hologram, phase differences less than the threshold $\pi/24$ radians are considered acceptable. At positions satisfying this criterion, a slot is introduced along the x-axis. The $\pi/24$ threshold value was selected by trial and error to properly approximate the desired aperture field distribution. A higher threshold value would result in defocusing due to imperfect constructive interference at the focal point; a lower threshold value would increase the phase accuracy of the hologram but can result in too few slots on the metasurface layer, causing higher sidelobe levels and aliasing. Using the calculated hologram (U) after thresholding, an illustration of the slot locations required to generate an on-axis focal spot is shown in Fig. 1 (a).

Though phase is traditionally more important in hologram design, the amplitude distribution across an antenna aperture is known to have significant effects on beam width and side lobes levels [55]. For a focused aperture, it is important to have all the power focused in the main beam or main lobe. Reduction of the sidelobe levels in aperture design is a well-known problem, which can be overcome by using tapering of the coupling strength of the slots to the reference wave through varying the element geometry [47]–[50]. The coupling distribution in a phase-only hologram metasurface aperture design would be flat; all the elements are identical and couple the same percentage of incident power to free space. To reduce the sidelobe levels, we can apply a taper to the coupling distribution, which will directly affect the effective magnetic surface current distribution on the aperture. The coupling distribution we consider here has lower coupling at the edge of the aperture and gradually increases as we approach the center of the aperture. This tapering resembles the well-known triangle tapering in antenna engineering. If the elements near the edge have greater coupling strength, the reference wave will be depleted before reaching the central elements causing aliasing and higher sidelobes. It is also important to make sure the coupling is not too small overall because the guided mode would not decay before it reaches the center of the aperture (causing the guided wave to significantly vary from the model in Eq. (1)). It is important to emphasize that a more intelligent design can be found if the complete interactions between the slots and the guided wave is incorporated in the design model. This problem, which can be vital to designing electrically large holograms, will be addressed in future works.

III. RESULTS

To validate the proposed design and operation, we develop two different samples: one with tapering and the other without. The bilayer structure was designed using low-loss, 1.524-mm-thick Rogers 3003 copper-clad circuit board substrate ($\varepsilon_r = 3.00$ and $\tan\delta = 0.001$). The aperture was designed to operate at 20 GHz in the K-band. Accounting for the limitations of in-house fabrication and simulation time, the aperture size was chosen to be a modest 10 cm in diameter (D). The inner diameter of the annular ring (D_{Ring}) coupling the two layers is selected to be 8.9 cm. Larger apertures can easily be manufactured by more advanced fabrication facilities or can be assembled by tiling many smaller apertures with precision alignment.

Here, we consider a focal spot located along the optical axis at F (0 cm, 0 cm, 10 cm). The slot dimensions were chosen by simulating a single slot in CST Microwave Studio, in a similar fashion as in [56]. The slot was designed in a parallel plate geometry where a 1.524-mm-thick Rogers 3003 substrate is sandwiched between two copper plates as shown in the inset of Fig. 2. The resonant frequencies (21–23GHz) of the slots are intentionally selected to be shifted from the operating frequency (20 GHz) so that the elements are not strongly coupled to the guided mode. Strongly coupled elements can

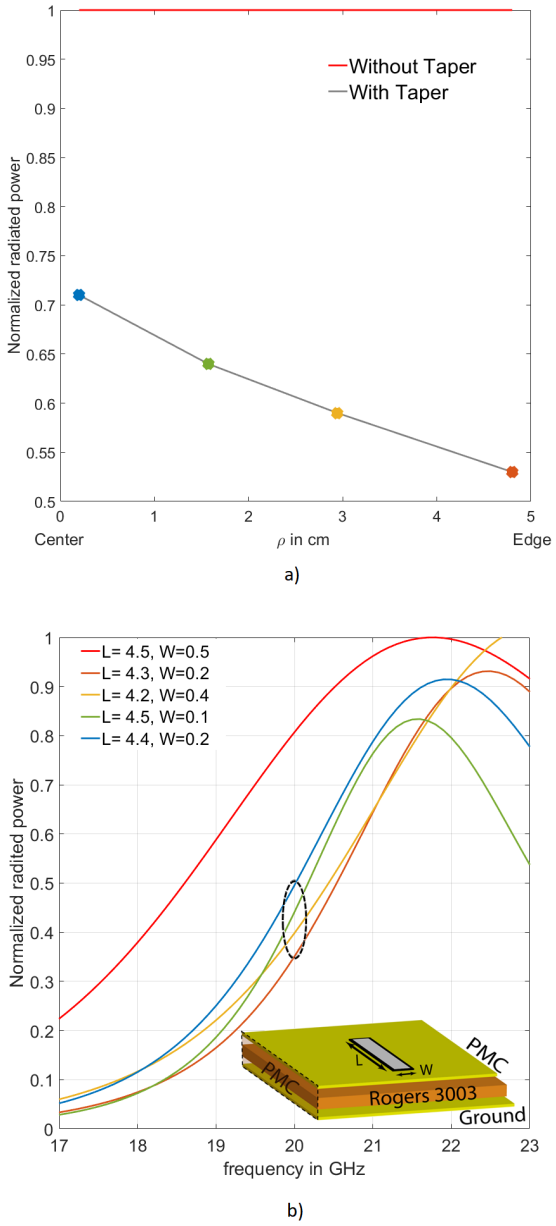

FIGURE 2. a) Coupling distribution for the metasurface aperture with and without tapering b) Power radiated for different slot dimension used for the design with taper (schematic of the unit cell in the inset).

perturb the waveguide mode and interact strongly with each other. The slot length of 4.5 mm and width of 0.5 mm was selected for the design without tapering. For the design with tapering, the slot length and width are jointly varied from 4.1 to 4.6 mm and 0.1 to 0.5 mm. A coupling distribution, which results in a gradual increase in the coupling towards the center of the aperture, is presented in Fig. 2(a). The coupling distribution is found by calculating the power radiated from each slot in the full wave simulations, as shown in Fig. 2(b). The plots in Fig. 2 report the normalized radiated power for the different slot widths and lengths used for the tapering design. The same coloring scheme is used for both plots of Fig. 2. During the process of designing the slots, it is ensured

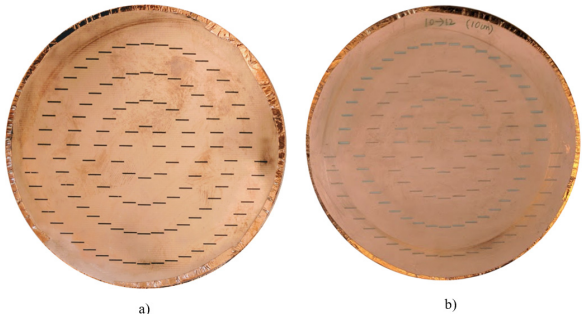

FIGURE 3. Assembled fabricated sample with copper tape covering the edges a) on-axis untapered b) tapered aperture.

that the resonant frequencies of the slots are away from the operating frequency (20 GHz).

To fabricate the metasurface focusing apertures, we patterned the desired collection of slots on the top copper layer of a one-sided, copper-clad Roger 3003 substrate using a U3 LPKF laser milling system. Figure 3 shows the assembled designs. For each design, the metasurface and the feed layer are aligned along their edges. The edges are covered using a copper tape to provide a cavity structure and clamps are employed around the aperture's edge to ensure that there is no gap between the two layers. While this is sufficient for the proof-of-concept structures presented here, future devices can use binding mechanisms to attach the two layers together.

We first measured the reflection coefficients of both the untapered and tapered designs and found them to be -16.1 dB and -18.5 dB respectively. The percentage bandwidth over which the reflection coefficients stay below -10 dB are 0.78% and 0.9% respectively for the untapered and tapered designs (assuming operating frequency of 20 GHz). It is important to note that the shape of the focal spot changes as the driving frequency moves away from the design frequency. The narrowband operation observed here is in fact desired in many applications involving near field focusing to avoid interference concerns.

To measure the field radiated from the metasurface aperture we used a planar near-field scanning system (NSI 200 V–3x3). The near-field scan of the aperture is performed at the focal plane (located at $z_0 = 10$ cm) using a WR-42 open-ended rectangular waveguide. The field measurement in this manner can be used to generate the fields everywhere in the Fresnel zone and far field of the aperture [57]. For example, to produce fields at a different distance, we first backpropagate the measured near field scan to the aperture plane and subsequently forward propagate to all locations in the range.

We first examine the field profile at the focal plane ($z_0 = 10$ cm) in the cross-range direction. This field intensity is plotted in Fig. 4 for the different structures and for three different cases: analytical, simulated, and experimental. In the analytical case, we model the slots as magnetic dipoles whose complex amplitudes are determined by the x-component of

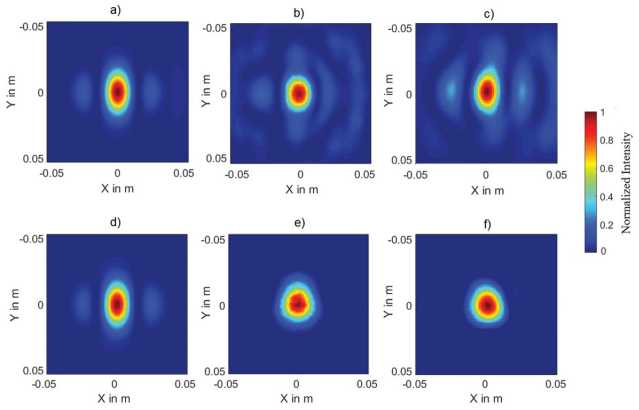

FIGURE 4. Normalized cross-range electric field intensity (linear scale) patterns of the metasurface aperture at the focal plane $z_0 = 10$cm (a) analytical (untapered) (b) CST microwave studio (untapered) (c) experimental (untapered) (d) analytical (tapered) (e) CST microwave studio (tapered) (f) experimental (tapered).

the guided magnetic field, as described in Section II [53]. The fields from the slots are then propagated and summed to determine the fields in the focusing region. We note that the decay of the guided wave due to the radiation from the slots is not modeled in our current analytical calculations. The mutual coupling between the slots, which is also not accounted for in the current analytical modeling, may have additional small effects on the focal properties. This interaction and the decay of the guided wave due to radiation from the slots will be accounted for in future works by incorporating a self-consistent dipolar formulation [54], [58], [59]. The simulated case represents the fields from the designed aperture using the commercial full-wave solver, CST Microwave Studio. The experimental plot corresponds to the results obtained using post-processing of near field scanned data (as outlined above). Examining the cross-range plots in Fig. 4, a focal spot is evident in both the tapered and the untapered designs. Figure 4 (a-c) represents the design without tapering, where it is evident that the experimental results exhibit higher side lobes when compared to the analytical results. To reduce the sidelobe levels the coupling distribution described in Fig. 2 is applied and the resulting reduced sidelobes are seen in Fig. 4 (d-f).

To quantitatively compare the focusing performance of the fabricated samples, we define a focusing efficiency as the amount of power in the focal spot to the total power at the focal plane. This quantity is calculated to be 40.1% and 52.3% for the untapered and tapered designs, respectively, clearly demonstrating the efficiency of the tapered design to confine the field in the prescribed focal spot.

Next, we present the 1-D point spread function analysis of the analytical, simulated, and experimental results to quantify the focusing capabilities of the designed holographic metasurface apertures. The resulting 1-D focal patterns are plotted in Fig. 5 along the x direction. Close agreement is seen between the experiments and simulations, verifying the proposed design for both the tapered and untapered designs.

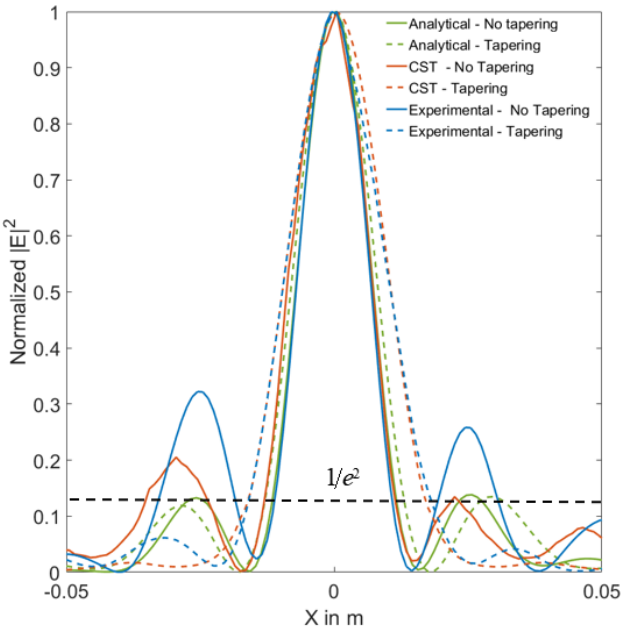

FIGURE 5. Normalized 1-D cross-range electric intensity (linear scale) patterns of the untapered (solid line) and tapered (dotted lines) metasurface aperture.

The sidelobe levels for the tapered design in simulation and experiment are seen in Fig. 5 (dotted lines) and are considerably lower compared to the untapered design (solid lines). The beam waist for the tapered design is slightly increased compared to the untapered design, which is a known and inevitable consequence for tapered apertures. An increase in the beam waist can be acceptable as the sidelobes have been substantially reduced, resulting in more power being concentrated in the main focus.

It is also worth noting that the focal spot size matches the predicted value from Gaussian optics [13] for the untapered design, calculated using the aperture dimensions, focal length, and wavelength of operation as given by

$$w_0 = \frac{4}{\pi} \frac{z_0 \lambda_0}{D \cos^2(\theta)} \tag{4}$$

Here, w_0 is the diameter of the spot at the focal plane, z_0 is the on-axis focal distance along the optical axis, λ_0 is the free space wavelength, and θ is the angle between the optical axis of the aperture and the vector defined from the aperture center to the position of the focus (0° for on-axis metasurface aperture). Table 1 provides a comparison of the spot size values obtained with the different methods for both

TABLE 1. Spot size calculations (cm).

	Gaussian Optics	Analytical	CST	Experimental
Spot size (Untapered)	2	2.3	2.3	2.2
Spot size (Tapered)	2	2.4	3.1	3.15

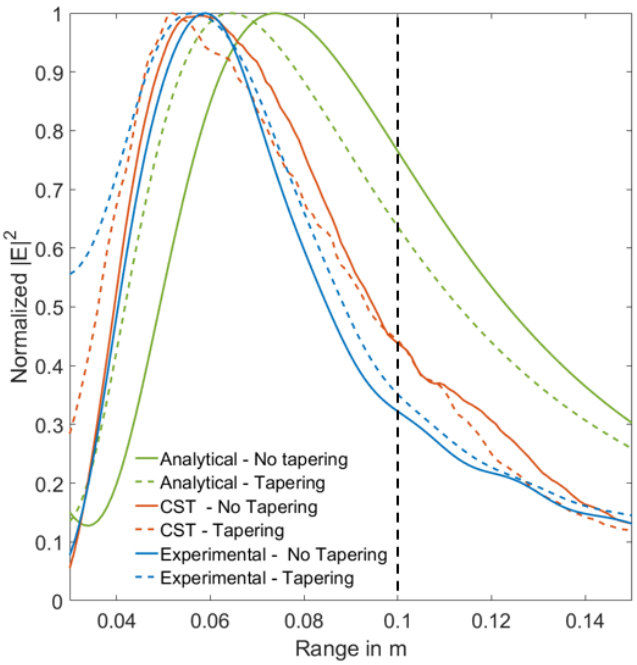

FIGURE 6. **Normalized 1-D range electric intensity (linear scale) patterns of the untapered (solid line) and tapered (dotted lines) metasurface aperture.**

the tapered and untapered design. The $1/e^2$ points obtained from Fig. 5 (black horizontal dotted line) correspond to the spot size of the metasurface aperture.

From the cross-range analysis shown above, it is evident that the focus is obtained at the desired focal plane z_0. We now analyze the fields in the range direction (along the optical axis). The experimental graphs are obtained by post processing of near field scanned data as outlined before. The 1-D range plots for the different structures (tapered and not tapered) and for the three different methods are presented in Fig. 6. The range plots are shown for distances larger than 3 cm ($2\lambda_0$) from the aperture because the fields close to the aperture ($<2\lambda_0$) contain evanescent components that are not considered in the analytical model and measured data [61]. We see that the fields generated by the hologram interfere constructively along the range to form the prescribed focus. However, the range plots in Fig. 6 reveal the fact that the peak intensity in the range does not occur at the intended focal plane (denoted by the black dotted line). Several other authors [62], [63] have noted this expected phenomenon. When a reference wave is diffracted by an aperture of finite dimension the point of maximum intensity is often not located at the intended geometrical focus but is closer to the aperture—a phenomenon commonly referred to as focal shift [62], [63]. In order to better understand the effects of the finite aperture size, let us denote s(x, y) as the ideal aperture field or hologram (produced by the hypothetical source at $F(x_0, y_0, z_0)$). This ideal aperture field distribution is truncated by the finite size of the metasurface, denoted by $t(x, y)$, where $t(x, y) = 1$ for $\sqrt{x^2 + y^2} \leq D/2$ and is zero otherwise. The fields in the spatial frequency domain are given by the convolution $S(k_x, k_y) \otimes T(k_x, k_y)$, where S is the ideal angular spectrum, T is the aperture angular spectrum and $\otimes$ indicates the convolution operation. As a result, only certain spectral components are transmitted and the components truncated by the finite size of the aperture will result in the shift of the focus towards the aperture. This explanation means a larger aperture would result in a smaller focal shift. To better quantify this problem in the design process, a unitless parameter called the Fresnel number can be considered [61]. The Fresnel number of a system with the largest dimension (D) is given by $N = D^2/\lambda_0 z_0$. In the current design, the Fresnel number N is equal to 6.66 which is relatively low [62]. In future works, the difficulties associated with small Fresnel number can be overcome by using a larger aperture or by operating at higher frequencies. It is also worth noting that the tapering slightly deteriorates the focal shift. This is expected from the analysis above; for a tapered aperture, t(x,y) is not 1 uniformly, which results in further filtering of the spatial components.

IV. CONCLUSION

This paper shows the potential to focus electromagnetic fields to desired spots with linear polarization using metasurface holograms. The proposed design and operation were confirmed via simulations and experiments in the K-band frequency range. To highlight the flexibility of this method, two different linearly polarized near-field focusing metasurface apertures were designed, one without tapering and another with tapering to reduce the sidelobe levels. Full-wave simulations, experimental analysis, and analytical predictions for the tapered aperture showed substantially smaller sidelobes when compared with the aperture design without tapering. The demonstrated focusing metasurface holds promise as the building block for wireless power transfer in the Fresnel zone, as suggested in [13].

The proposed design has plenty of room for further development. The design can be extended to achieve focusing in both polarizations and off-axis focusing. In this paper, narrow slots are used as the radiating elements of the hologram, but they can be replaced by efficient, reconfigurable metamaterial cells [52], [64] paving the path toward a steerable focal spot. The proposed design can also be scaled to higher frequencies, where electrically large apertures can be easily fabricated without becoming cumbersome. In the current design process of the metasurface, the element-to-element interactions have not been considered; the discrete dipole approximation [58]–[60] method can be used in future works to account for such interactions. Lastly, the analytical prediction of the sidelobe levels at the focal plane can be improved by means of a self-consistent dipolar formulation to optimize the coupling distribution across the aperture. The cavity-backed metasurface aperture proposed here can support tunable metamaterial structures resulting in dynamically reconfigurable metasurfaces that have the potential to be developed into a powerful source for Fresnel zone wireless power transfer.

REFERENCES

[1] F. Tofigh, J. Nourinia, M. Azarmanesh, and K. M. Khazaei, "Near-field focused array microstrip planar antenna for medical applications," *IEEE Antennas Wireless Propag. Lett.*, vol. 13, pp. 951–954, 2014.

[2] M. Bogosanovic and A. G. Williamson, "Microstrip antenna array with a beam focused in the near-field zone for application in noncontact microwave industrial inspection," *IEEE Trans. Instrum. Meas.*, vol. 56, no. 6, pp. 2186–2195, Dec. 2007.

[3] K. D. Stephan, J. B. Mead, D. M. Pozar, L. Wang, and J. A. Pearce, "A near field focused microstrip array for a radiometric temperature sensor," *IEEE Trans. Antennas Propag.*, vol. 55, no. 4, pp. 1199–1203, Apr. 2007.

[4] J. S. Ho *et al.*, "Wireless power transfer to deep-tissue microimplants," *Proc. Nat. Acad. Sci. USA*, vol. 111, no. 22, pp. 7974–7979, Apr. 2014.

[5] S. Kim, J. S. Ho, and A. S. Poon, "Midfield wireless powering of subwavelength autonomous devices," *Phys. Rev. Lett.*, vol. 110, no. 20, p. 203905, 2013.

[6] J. T. Loane, III, and S.-W. Lee, "Gain optimization of a near-field focusing array for hyperthermia applications," *IEEE Trans. Microw. Theory Techn.*, vol. 37, no. 10, pp. 1629–1635, Oct. 1989.

[7] N. Tesla, "Apparatus for transmitting electrical energy," Google Patents 1 119 732 A, Dec. 1, 1914.

[8] A. Kurs, A. Karalis, R. Moffatt, J. D. Joannopoulos, P. Fisher, and M. Soljačić, "Wireless power transfer via strongly coupled magnetic resonances," *Science*, vol. 317, no. 5834, pp. 83–86, 2007.

[9] A. P. Sample, D. T. Meyer, and J. R. Smith, "Analysis, experimental results, and range adaptation of magnetically coupled resonators for wireless power transfer," *IEEE Trans. Ind. Electron.*, vol. 58, no. 2, pp. 544–554, Feb. 2011.

[10] B. Wang, W. Yerazunis, and K. H. Teo, "Wireless power transfer: Metamaterials and array of coupled resonators," *Proc. IEEE*, vol. 101, no. 6, pp. 1359–1368, Jun. 2013.

[11] G. V. Borgiotti, "Maximum power transfer between two planar apertures in the Fresnel zone," *IEEE Trans. Antennas Propag.*, vol. 14, no. 2, pp. 158–163, Mar. 1966.

[12] L. Shan and W. Geyi, "Optimal design of focused antenna arrays," *IEEE Trans. Antennas Propag.*, vol. 62, no. 11, pp. 5565–5571, Nov. 2014.

[13] D. R. Smith *et al.*, "An analysis of beamed wireless power transfer in the Fresnel zone using a dynamic, metasurface aperture," *J. Appl. Phys.*, vol. 121, no. 1, p. 014901, 2017.

[14] A. Massa, G. Oliveri, F. Viani, and P. Rocca, "Array designs for long-distance wireless power transmission: State-of-the-art and innovative solutions," *Proc. IEEE*, vol. 101, no. 6, pp. 1464–1481, Jun. 2013.

[15] V. R. Gowda, O. Yurduseven, G. Lipworth, T. Zupan, M. S. Reynolds, and D. R. Smith, "Wireless power transfer in the radiative near field," *IEEE Antennas Wireless Propag. Lett.*, vol. 15, pp. 1865–1868, 2016.

[16] A. Buffi, A. A. Serra, P. Nepa, and G. Manara, "A focused planar microstrip array for 2.4 GHz RFID readers," *IEEE Trans. Antennas Propag.*, vol. 58, no. 5, pp. 1536–1544, May 2010.

[17] H.-T. Chou, T.-M. Hung, N.-N. Wang, H.-H. Chou, C. Tung, and P. Nepa, "Design of a near-field focused reflectarray antenna for 2.4 GHz RFID reader applications," *IEEE Trans. Antennas Propag.*, vol. 59, no. 3, pp. 1013–1018, Mar. 2011.

[18] Y. Li and V. Jandhyala, "Design of retrodirective antenna arrays for short-range wireless power transmission," *IEEE Trans. Antennas Propag.*, vol. 60, no. 1, pp. 206–211, Jan. 2012.

[19] T. Okuyama, Y. Monnai, and H. Shinoda, "20-GHz focusing antennas based on corrugated waveguide scattering," *IEEE Antennas Wireless Propag. Lett.*, vol. 12, pp. 1284–1286, 2013.

[20] P. del Hougne, M. Fink, and G. Lerosey. (2017). "Shaping microwave fields using non-linear unsolicited feedback: Application to enhanced energy harvesting." [Online]. Available: https://arxiv.org/abs/1706.00450

[21] N. Kaina, M. Dupré, G. Lerosey, and M. Fink, "Shaping complex microwave fields in reverberating media with binary tunable metasurfaces," *Sci. Rep.*, vol. 4, Oct. 2014, Art. no. 6693.

[22] D. Arnitz and M. S. Reynolds, "MIMO wireless power transfer for mobile devices," *IEEE Pervasive Comput.*, vol. 15, no. 4, pp. 36–44, Oct. 2016.

[23] R. C. Hansen, *Phased Array Antennas*, vol. 213. Hoboken, NJ, USA: Wiley, 2009.

[24] R. Siragusa, P. Lemaître-Auger, and S. Tedjini, "Tunable near-field focused circular phase-array antenna for 5.8-GHz RFID applications," *IEEE Antennas Wireless Propag. Lett.*, vol. 10, pp. 33–36, 2011.

[25] F. C. Williams and W. H. Kummer, "Electronically scanned antenna," Google Patents 4 276 551 A, Jun. 30, 1981.

[26] H. D. Hristov, "Fresnal zones in wireless links," in *Zone Plate Lenses and Antennas*. Norwood, MA, USA: Artech House, 2000.

[27] S. Karimkashi and A. A. Kishk, "Focusing properties of Fresnel zone plate lens antennas in the near-field region," *IEEE Trans. Antennas Propag.*, vol. 59, no. 5, pp. 1481–1487, May 2011.

[28] D. Blanco, J. L. Gómez-Tornero, E. Rajo-Iglesias, and N. Llombart, "Holographic surface leaky-wave lenses with circularly-polarized focused near-fields—Part II: Experiments and description of frequency steering of focal length," *IEEE Trans. Antennas Propag.*, vol. 61, no. 7, pp. 3486–3494, Jul. 2013.

[29] M. Ettorre, S. C. Pavone, M. Casaletti, and M. Albani, "Experimental validation of Bessel beam generation using an inward Hankel aperture distribution," *IEEE Trans. Antennas Propag.*, vol. 63, no. 6, pp. 2539–2544, Jun. 2015.

[30] J. D. Heebl, M. Ettorre, and A. Grbic, "Wireless links in the radiative near field via Bessel beams," *Phys. Rev. Appl.*, vol. 6, no. 3, p. 034018, Sep. 2016.

[31] I. Iliopoulos, M. Casaletti, R. Sauleau, P. Pouliguen, P. Potier, and M. Ettorre, "3-D shaping of a focused aperture in the near field," *IEEE Trans. Antennas Propag.*, vol. 64, no. 12, pp. 5262–5271, Dec. 2016.

[32] M. F. Imani and A. Grbic, "An experimental concentric near-field plate," *IEEE Trans. Microw. Theory Techn.*, vol. 58, no. 12, pp. 3982–3988, Dec. 2010.

[33] M. F. Imani and A. Grbic, "Unidirectional wireless power transfer using near-field plates," *J. Appl. Phys.*, vol. 117, no. 18, p. 184903, 2015.

[34] D. Blanco, J. L. Gomez-Tornero, E. Rajo-Iglesias, and N. Llombart, "Radially polarized annular-slot leaky-wave antenna for three-dimensional near-field microwave focusing," *IEEE Antennas Wireless Propag. Lett.*, vol. 13, pp. 583–586, 2014.

[35] A. J. Martinez-Ros, J. L. Gomez-Tornero, F. J. Clemente-Fernandez, and J. Monzo-Cabrera, "Microwave near-field focusing properties of width-tapered microstrip leaky-wave antenna," *IEEE Trans. Antennas Propag.*, vol. 61, no. 6, pp. 2981–2990, Jun. 2013.

[36] Y. Monnai and H. Shinoda, "Focus-scanning leaky-wave antenna with electronically pattern-tunable scatterers," *IEEE Trans. Antennas Propag.*, vol. 59, no. 6, pp. 2070–2077, Jun. 2011.

[37] C. L. Holloway, E. F. Kuester, J. A. Gordon, J. O'Hara, J. Booth, and D. R. Smith, "An overview of the theory and applications of metasurfaces: The two-dimensional equivalents of metamaterials," *IEEE Antennas Propag. Mag.*, vol. 54, no. 2, pp. 10–35, Apr. 2012.

[38] M. C. Johnson, S. L. Brunton, N. B. Kundtz, and J. N. Kutz, "Sidelobe canceling for reconfigurable holographic metamaterial antenna," *IEEE Trans. Antennas Propag.*, vol. 63, no. 4, pp. 1881–1886, Apr. 2015.

[39] K. M. Palmer, "Metamaterials make for a broadband breakthrough," *IEEE Spectr.*, vol. 49, no. 1, pp. 13–14, Jan. 2012.

[40] D. F. Sievenpiper, J. H. Schaffner, H. J. Song, R. Y. Loo, and G. Tangonan, "Two-dimensional beam steering using an electrically tunable impedance surface," *IEEE Trans. Antennas Propag.*, vol. 51, no. 10, pp. 2713–2722, Oct. 2003.

[41] B. H. Fong, J. S. Colburn, J. J. Ottusch, J. L. Visher, and D. F. Sievenpiper, "Scalar and tensor holographic artificial impedance surfaces," *IEEE Trans. Antennas Propag.*, vol. 58, no. 10, pp. 3212–3221, Oct. 2010.

[42] S. Larouche, Y.-J. Tsai, T. Tyler, N. M. Jokerst, and D. R. Smith, "Infrared metamaterial phase holograms," *Nature Mater.*, vol. 11, no. 5, pp. 450–454, 2012.

[43] G. Lipworth, N. W. Caira, S. Larouche, and D. R. Smith, "Phase and magnitude constrained metasurface holography at W-band frequencies," *Opt. Exp.*, vol. 24, no. 17, pp. 19372–19387, 2016.

[44] M. Ando, T. Numata, J.-I. Takada, and N. Goto, "A linearly polarized radial line slot antenna," *IEEE Trans. Antennas Propag.*, vol. 36, no. 12, pp. 1675–1680, Dec. 1988.

[45] M. Ando, K. Sakurai, N. Goto, K. Arimura, and Y. Ito, "A radial line slot antenna for 12 GHz satellite TV reception," *IEEE Trans. Antennas Propag.*, vol. 33, no. 12, pp. 1347–1353, Dec. 1985.

[46] M. I. Imran and A. R. Tharek, "Radial line slot antenna development for outdoor point to point application at 5.8 GHz band," in *Proc. RF Microw. Conf. (RFM)*, Oct. 2004, pp. 103–105.

[47] A. Akiyama, T. Yamamoto, M. Ando, N. Goto, and E. Takeda, "Design of radial line slot antennas for millimeter wave wireless LAN," in *Antennas Propag. Soc. Int. Symp. Dig.*, vol. 4. Jul. 1997, pp. 2516–2519.

[48] M. Ando, K. Sakurai, and N. Goto, "Characteristics of a radial line slot antenna for 12 GHz band satellite TV reception," *IEEE Trans. Antennas Propag.*, vol. 34, no. 10, pp. 1269–1272, Oct. 1986.

[49] M. Ettorre *et al.*, "On the near-field shaping and focusing capability of a radial line slot array," *IEEE Trans. Antennas Propag.*, vol. 62, no. 4, pp. 1991–1999, Apr. 2014.
[50] T. Yamamoto, N. T. Chien, M. Ando, N. Goto, M. Hirayama, and T. Ohmi, "Design of radial line slot antennas at 8.3 GHz for large area uniform plasma generation," *Jpn. J. Appl. Phys.*, vol. 38, no. 4R, p. 2082, 1999.
[51] T. Sleasman, M. Boyarsk, M. F. Imani, J. N. Gollub, and D. R. Smith, "Design considerations for a dynamic metamaterial aperture for computational imaging at microwave frequencies," *J. Opt. Soc. Amer. B, Opt. Phys.*, vol. 33, no. 6, pp. 1098–1111, Jun. 2016.
[52] T. Sleasman, M. F. Imani, J. N. Gollub, and D. R. Smith, "Dynamic metamaterial aperture for microwave imaging," *Appl. Phys. Lett.*, vol. 107, no. 20, p. 204104, Nov. 2015.
[53] G. Lipworth *et al.*, "Comprehensive simulation platform for a metamaterial imaging system," *Appl. Opt.*, vol. 54, no. 31, pp. 9343–9353, 2015.
[54] L. M. Pulido-Mancera, T. Zvolensky, M. F. Imani, P. T. Bowen, M. Valayil, and D. R. Smith, "Discrete dipole approximation applied to highly directive slotted waveguide antennas," *IEEE Antennas Wireless Propag. Lett.*, vol. 15, pp. 1823–1826, 2016.
[55] C. A. Balanis, *Antenna Theory: Analysis and Design*. Hoboken, NJ, USA: Wiley, 2016.
[56] M. F. Imani, T. Sleasman, J. N. Gollub, and D. R. Smith, "Analytical modeling of printed metasurface cavities for computational imaging," *J. Appl. Phys.*, vol. 120, no. 14, p. 144903, 2016.
[57] A. D. Yaghjian, "An overview of near-field antenna measurements," *IEEE Trans. Antennas Propag.*, vol. 34, no. 1, pp. 30–45, Jan. 1986.
[58] P. T. Bowen, T. Driscoll, N. B. Kundtz, and D. R. Smith, "Using a discrete dipole approximation to predict complete scattering of complicated metamaterials," *New J. Phys.*, vol. 14, no. 3, p. 033038, 2012.
[59] M. Johnson, P. Bowen, N. Kundtz, and A. Bily, "Discrete-dipole approximation model for control and optimization of a holographic metamaterial antenna," *Appl. Opt.*, vol. 53, no. 25, pp. 5791–5799, 2014.
[60] L. Pulido-Mancera, P. T. Bowen, M. F. Imani, N. Kundtz, and D. Smith, "Polarizability extraction of complementary metamaterial elements in waveguides for aperture modeling," *Phys. Rev. B, Condens. Matter*, vol. 96, no. 23, p. 235402, 2017.
[61] D. Slater, *Near-Field Antenna Measurements*. Norwood, MA, USA: Artech House, 1991.
[62] Y. Li and E. Wolf, "Focal shift in focused truncated Gaussian beams," *Opt. Commun.*, vol. 42, no. 3, pp. 151–156, 1982.
[63] M. Martínez-Corral and V. Climent, "Focal switch: A new effect in low-Fresnel-number systems," *Appl. Opt.*, vol. 35, no. 1, pp. 24–27, 1996.
[64] I. Yoo, M. F. Imani, T. Sleasman, and D. R. Smith, "Efficient complementary metamaterial element for waveguide-fed metasurface antennas," *Opt. Exp.*, vol. 24, no. 25, pp. 28686–28692, 2016.

VINAY R. GOWDA received the B.E. degree in electrical and communication engineering from Visvesvaraya Technological University, Karnataka, India, in 2009, and the M.S. degree in electrical engineering from The University of Texas, Arlington, TX, USA, in 2011. From 2011 to 2014, he was a Hardware Engineer with Intel/Intel Labs, Folsom, CA, USA.

Since 2014, he has been with the Center for Metamaterials and Integrated Plasmonics, Duke University, Durham, NC, USA. He is currently a Graduate Student with the Department of Electrical and Computer Engineering. His current research interests include wireless power transfer, focused apertures, metamaterials, and RF design.

MOHAMMADREZA F. IMANI (M'08) received the B.S.E. degree from the Sharif University of Technology, Tehran, Iran, in 2007, and the M.S.E. and Ph.D. degrees from the University of Michigan, Ann Arbor, MI, USA, in 2010 and 2013, respectively, all in electrical engineering.

Since 2014, he has been a Post-Doctoral Associate with the Department of Electrical and Computer Engineering, Duke University, Durham, NC, USA. His research includes metamaterials and metasurfaces, microwave imaging and sensing, wireless power transfer, and communication systems.

TIMOTHY SLEASMAN (S'16) received the B.S. degree in mathematics and physics from the Boston College, Chestnut Hill, MA, USA, in 2013. He is currently pursuing the Ph.D. degree with the Department of Electrical and Computer Engineering, Duke University.

Since 2013, he has been with the Center for Metamaterials and Integrated Plasmonics, Duke University, Durham, NC, USA. He is currently a Graduate Student with the Department of Electrical and Computer Engineering. His current research interests include computational imaging, dynamically tunable metasurfaces, and novel hardware platforms for generating tailored electromagnetic wave fronts.

OKAN YURDUSEVEN (S'09–M'11–SM'16) received the B.Sc. and M.Sc. degrees from Yildiz Technical University, Istanbul, Turkey, in 2009 and 2011, respectively, and the Ph.D. degree from Northumbria University, Newcastle upon Tyne, U.K., in 2014, all in electrical engineering.

From 2009 to 2011, he was a Research Assistant with the Department of Electrical and Electronic Engineering, Marmara University, Istanbul, Turkey. From 2011 to 2014, he was a Lecturer (part-time) with the Faculty of Engineering and Environment, Northumbria University. Since 2014, he has been a Post-Doctoral Associate with the Center for Metamaterials and Integrated Plasmonics, Department of Electrical and Computer Engineering, Duke University, in collaboration with the U.S. Department of Homeland Security. His research interests include microwave and millimeter-wave imaging, multiple-input-multiple-output radar, wireless power transfer, antennas and propagation, antenna measurement techniques, and metamaterials. He has authored over 80 peer-reviewed technical journal and conference articles, and six provisional patents. He has organized and chaired numerous sessions in international symposiums and conferences, including the IEEE International Symposium on Antennas and Propagation and European Conference on Antennas and Propagation.

Dr. Yurduseven is a member of the European Association on Antennas and Propagation. He was a recipient of the Academic Excellence Award from the Association of British–Turkish Academics in London in 2013. He also received the Best Paper Award from the Mediterranean Microwave Symposium in 2012 and the Travel Award from the Institution of Engineering and Technology. He received the Duke Postdoctoral Professional Development Award in 2017. In 2017, he also received the Outstanding Postdoctoral Award from Duke University. He has been included in the Marquis Who's Who for Excellence in Research in 2017 and received the NASA Postdoctoral Program Fellowship (2017). He serves as a Reviewer for the IEEE TRANSACTIONS ON ANTENNAS AND PROPAGATION, the IEEE TRANSACTIONS ON MICROWAVE THEORY AND TECHNIQUES, the IEEE ANTENNAS AND WIRELESS PROPAGATION LETTERS, IEEE ACCESS, *Progress in Electromagnetics Research*, and *Applied Physics B*.

DAVID R. SMITH (M'98) received the Ph.D. degree in physics from the University of California at San Diego (UCSD) in 1994.

He is currently the Department Chair and the James B. Duke Professor of electrical and computer engineering with Duke University and the Director of the Center for Metamaterials and Integrated Plasmonics. He also holds the positions of adjunct professor with the Physics Department, UCSD, an Affiliate Faculty with the Electrical and Computer Engineering Department, University of Washington, and a Visiting Professor of physics with the Imperial College London, London. His research interests include the theory, simulation and characterization of unique electromagnetic structures, including photonic crystals and metamaterials, and applications of such materials.

While at UCSD, he and his colleagues demonstrated the first left-handed (or negative index) metamaterial at microwave frequencies in 2000. He has over 200 publications on matematerials and plasmonics, and was selected by ISI-Reuters as a ''Citation Laureate'' for the most number of ''highly cited'' papers in the field of physics over the last decade in 2009. He was once again recognized as one of the ''Highly Cited Researches 2014'' by ISI-Reuters in the category of physics.

Dr. Smith was elected as a member of The Electromagnetics Academy in 2002. In 2005, he was part of a five member team that received the Descartes Research Prize from the European Union, for their contributions to metamaterials and other novel electromagnetic materials. He also received the Stansell Research Award from the Pratt School of Engineering at Duke University in 2005. He was selected as one of the ''Scientific American 50,'' a group recognized by the Editors of Scientific American for Achievements in science, technology and policy in 2006. His work has twice appeared on the cover of Physics Today, and twice has been selected as one of the ''Top Ten Breakthroughs'' of the year by Science Magazine. He was a co-recipient of the James C. McGroddy Prize for New Materials at the American Physical Society in 2013.

In 2006, he, along with colleague Sir J. Pendry, suggested metamaterials could be used to design an electromagnetic cloak, introducing the new design tool of ''transformation optics.'' He was asked to write an op-ed piece for the New York Times on cloaking research in 2013.

In 2013, he served as the Founding and an Acting Director of the Metamaterials Commercialization Center (MCC), a unit within the Intellectual Ventures, Bellevue, WA, USA, dedicated to commercializing metamaterials concepts. MCC has, thus, far produced three spin out companies—Kymeta Corporation, Redmond, WA, USA, Evolv Technologies, Waltham, MA, USA, and Echodyne, Bellevue, WA, USA. He serves on the Advisory Board for Kymeta, which targets metamaterial-based antennas for satellite communications, and is a Co-Founder of Evolv Technologies, which targets metamaterial apertures for security screening applications, and Echodyne, which is seeking to apply metamaterial apertures to radar applications.